Accepted Manuscript

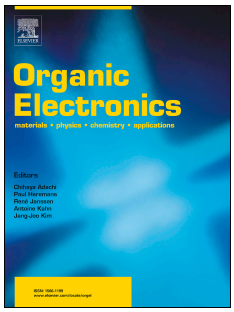

High efficiency small molecule-based donor materials for organic solar cells

Rashid Ilmi, Ashanul Haque, M.S. Khan

PII: S1566-1199(18)30155-1

DOI: 10.1016/j.orgel.2018.03.048

Reference: ORGELE 4606

To appear in: *Organic Electronics*

Received Date: 29 November 2017

Revised Date: 29 January 2018

Accepted Date: 27 March 2018

Please cite this article as: R. Ilmi, A. Haque, M.S. Khan, High efficiency small molecule-based donor materials for organic solar cells, *Organic Electronics* (2018), doi: 10.1016/j.orgel.2018.03.048.

Graphical abstract

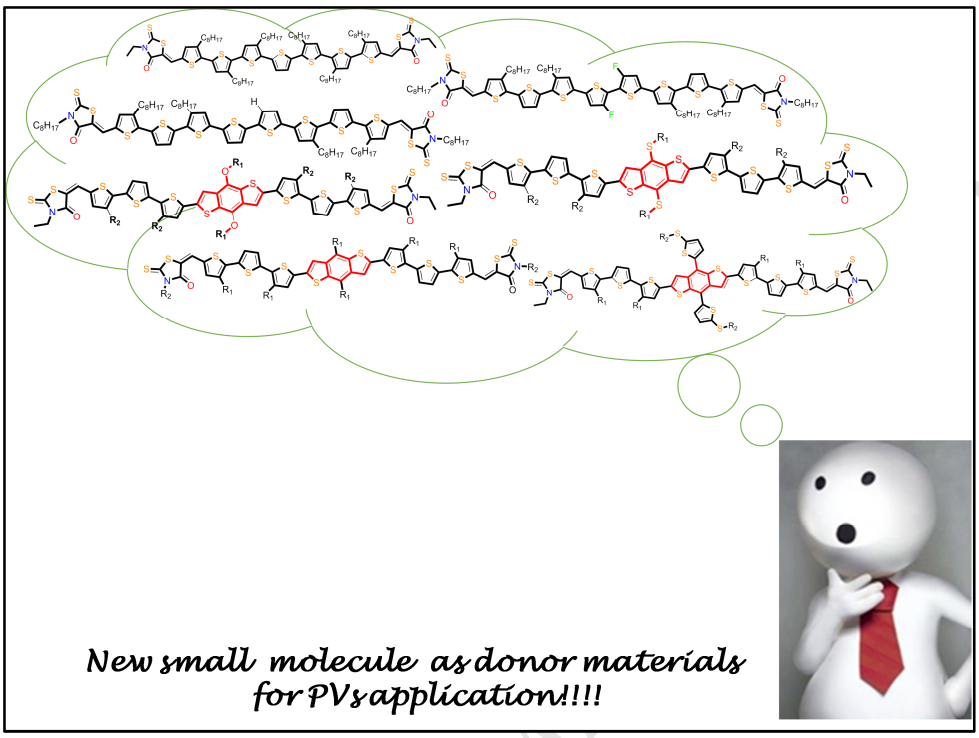

High Efficiency Small Molecule-Based Donor Materials for Organic Solar Cells

Rashid Ilmi, Ashanul Haque, M. S. Khan*

Department of Chemistry, Sultan Qaboos University, Al-Khod, Sultanate of Oman.

*Corresponding author: E-mail: msk@squ.edu.om
msk.squ.edu@gmail.com

. Tel: +968 2414 1493;
Fax: +968 2414 1469

Abstract:

Organic photovoltaic (OPV) materials, especially small molecule donor materials (SMDMs) have enormous potential to revolutionize the solar energy sector. However, to be a viable alternative to the polymer donor counterparts for commercialization, the SMDMs must have high power conversion efficiency (PCE). A large number of different SMDMs have been reported as active layers, which have crossed the 10% threshold of the PCE for commercialization. In this review, we present the SMDMs that have been developed in very recent years generating moderate to high-efficiency photovoltaic devices. The steady rise in PCE values in recent years and the variety of materials producing high PCEs point to a bright future for SMDMS as solar energy materials.

Keywords: Small molecule donor; Active layer; Molecular design.

1. Introduction

Solar energy is one of the most powerful alternatives to non-renewable fossil fuels. Unfortunately, we are unable to harness the full potential of the solar energy, partially due to engineering challenges and largely due to the lack of efficient photovoltaic (PV) cells, which convert sun light to electrical energy. Based on the solid-state electronic material system used, a PV cell can be divided into crystalline elemental (silicon), organic, thin-film (CIGS, CdTe, amorphous Si) or hybrid [1]. At present, the PV market is dominated (> 90%) by the crystalline, polycrystalline and amorphous inorganic materials based solar cells [2]. Despite the fact that these solar cells (SCs) have excellent light to electricity conversion ability, their high manufacturing cost, slow manufacturing, sensitivity to impurities, low-flexibility, etc. pose significant challenges to the industrial and individual consumers [3]. To overcome these challenges, organic photovoltaic (OPV) cells emerged as a promising alternative. Organic semiconductors are conjugated materials that conduct electricity when they reach sufficient number of alternating single and double bonds and have conductivity between a metal and an insulator (10^{-9} to 10^{3} Ω^{-1} cm^{-1}) [4]. Organic materials have several advantages over inorganic semiconductors like high absorption coefficient and broad absorption range, which can be tuned by chemical functionalization. The easy functionalization of organic semiconductors is a prime advantage that surpasses all advantages of inorganic semiconducting materials. The last decade witnessed a tremendous rise in the development of the OPVs with a high power conversion efficiency (PCE) [5] using organic donor material. Although this value is lower than their inorganic counterparts, it's sufficient for use, which is set at 10% [6].

Based on the type of molecular system used, OPV is divided into two classes: polymer-donor solar cells (PDSCs) and small molecule-donor solar cells (SMDSCs). Interestingly, the efficiency of SMDSCs have increased considerably from 0.001% in 1975 [7], through 1% in 1986 [8] to > 11.3% in 2017 [9, 10], which is very close to the highest value obtained by any OPV cells (PDSCs ~ 13%) [11]. This incredible rise in performance efficiency has been possible due to several advantages offered by the SMDMs, e.g., synthetic ease, synthetic reproducibility with high purity, discrete molecular weight, well defined molecular structure, low weight and cost, mechanical flexibility, suitability for large area applications and high charge carrier mobility, etc. [12-14]. Considering the importance of this rapidly developing field, we present herein the progress made in recent years in the development of SMDMs for OPV. **Figure 1** depicts result generated by Web of Science when searched for the term ''Organic Small Molecule Solar Cells" during the time interval of 2010–2017. A total of 553 articles have been published since the beginning of 21st century, which is still on the rise. Furthermore, citation related to this topic has also grown tremendously. Both PDSCs and

SMDSCs have been reported in the literature. In the succeeding sections, attempts have been made to discuss progress made in the development of SMDSCs for OPV.

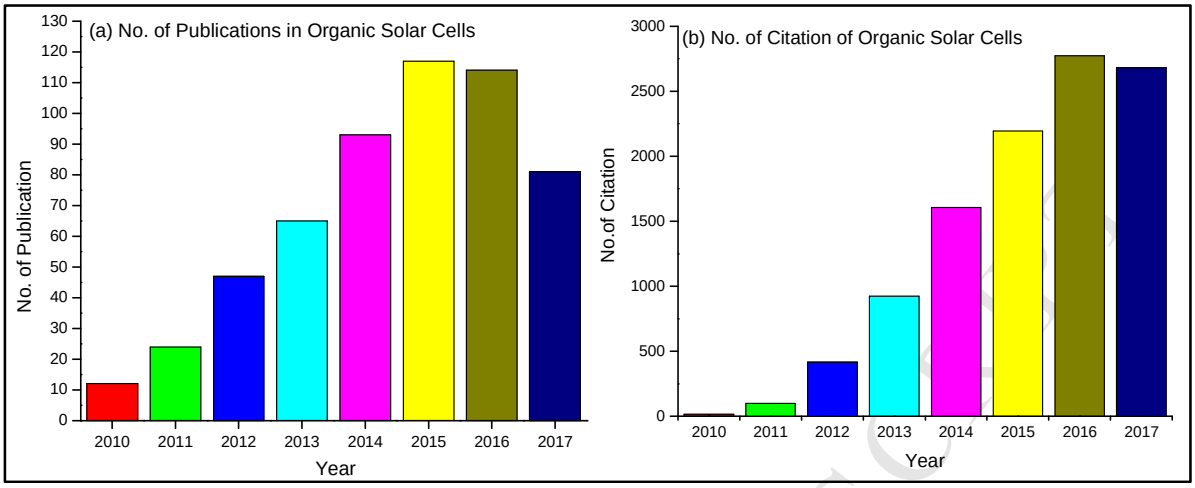

Figure 1: Histogram showing the number of scientific publications contributing to the subject "Organic SC(s)" by year. The period was **2010** - **2017** and the keyword was Organic Small Molecule Solar Cells. Search done through ISI, Web of Science.

2. Performance parameters of Solar Cells (SCs)

There are many excellent research articles and books which chronicles the structure and mechanism of PV devices [15-20]. We herein discuss briefly the performance parameters that are required for characterizing SCs. The OSCs are characterized under a 1000 W/m^2 light with the spectrum matching that of the sun on the earth's surface at an incident angle of 48.2° called the AM 1.5 spectrum [21]. A typical current–voltage (I-V) curve of a SC in the dark and under illumination are shown in **Figure 2a** along with the structures of standard PV cells (Figure 2b and 2c). In the dark, there is almost no current until the forward bias for voltages is larger than the open circuit voltage. Under illumination, the SCs start generating power which is recorded with a source meter. For characterization of any SC, the key parameter is the power conversion efficiency (PCE), which is the ratio of the maximum electrical power (P_m) generated by the device to the total incident optical power (P_{in}) (equation 1). P_{in} is given by the spectral intensity matching the sun's intensity on the Earth at an angle of 48.2 ° (equivalent to AM 1.5 spectrum) [22].

$$\eta_e = \frac{P_m}{P_{in}} \times 100 = \frac{V_{OC} \times I_{SC} \times FF}{P_{in}} \times 100 \qquad \textit{Eq. 1}$$

The term V_{oc} in Eq. (1) is open-circuit potential/voltage (V_{oc}) defined as the potential at which current is zero and depends on HOMO and LUMO energy level difference of the donor (D) and acceptor (A). Therefore, the V_{oc} of the SC can be increased either by reducing the HOMO level of the D or increasing the LUMO level of the A material. The second term in Eq. (1) is the J_{sc}, short-circuit current density and is a maximum generated photocurrent density. As the band-gap of the material decreases, the J_{sc} increases and can also be affetcted by

the electron and hole transport efficiency of the active material [23]. The third term is the fill factor (FF) and is the ratio of observed maximum power output to the theoretical power output. Maximum power output is given by P_m (= I_m x V_m), and the theoretical output is the product of J_{sc} and V_{oc} and therefore the FF can be defined by Eq. (**2**).

$$FF = \frac{J_{MP} \times V_{MP}}{J_{SC} \times V_{OC}} \qquad Eq.\ 2$$

The FF suggests how swiftly the charges can be removed from the cells and in an ideal case the value is 1.0. There are a number of factors that can affect the FF of SCs and they often interact in intricate ways. The series resistance (R_s), parallel resistance (R_{sh}) are two other important factors that affect the FF and performance of SCs. The physical phenomena governing J_{sc} [24, 25] and V_{oc} [26-28] have been well documented. However, the governance of the FF is still not so well documented and not so clearly understood [29].

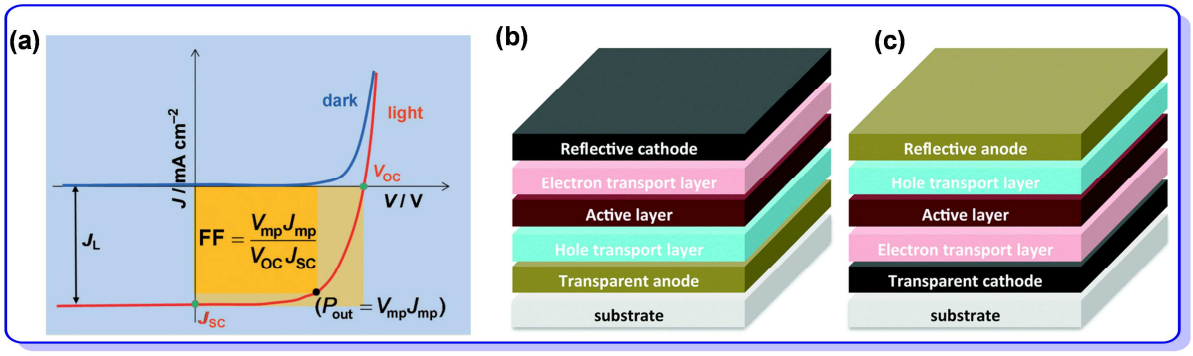

Figure 2. (a) A typical current-voltage *J-V* characteristics of solar cells reprinted with the permission of Ref. [30]. (b) standard architecture of bulk-heterojunction (BHJ) and (c) inverted structure.

3. SMDMs–based Photovoltaics

Several reviews have chronicled the progress made on SMDMs–based PV cells [30, 31]. Herein we have reviewed only very recent articles with moderate to high PCE.

3.1. Oligothiophene-based SMDMs

During the literature survey, we noted that most of SMDMs are based on electron-rich thiophene units, supporting the importance of this heterocyclic moiety in materials science. Sulfur containing heterocycles such as simple thiophene, fused and non-fused thiophenes, and their derivatives are commonly employed as electron-donor units in the small molecular donors. The electronic properties and bulk-heterojunction (BHJ) SC parameters of some recently reported oligothiophene based SMDMs are summarized in **Table 1**. The results indicate that structurally simple SMDMs molecules are potential donor candidates for achieving highly efficient OSCs. Liu *et al*. [32] reported an oligo-thiophene (n = 7) based small donor **1** (Chart 1) composed of 3-octylthiophene as the central donor unit decorated with 3-ethylrhodanine at the periphery. The electron withdrawing nature of 3-ethylrhodanine created a strong donor-acceptor (D-A) interaction within the oligomer, leading to absorption

in visible region and a low band gap (E_g^o) of 1.72 eV. Oligomer **1** produced high quality thin film through solution processing technique and showed broad absorption in visible region (450-750 nm) with λ_{max} = 618 nm with red-shift of ~ 110 nm compared to parent molecule **1** in chloroform ($CHCl_3$). Using **1** as donor and $PC_{61}BM$ as acceptor (Chart 1), they achieved a high PCE (6.10%) with V_{oc} of 0.92 V and J_{sc} of 13.98 mA/cm^2. An increase in the number of thiophene units in the central core (n = 8) with elongation of alkyl chain at the termini (**2**, Chart 1) did not affect the PV factors too much. However, a significant improvement in the PCE and other parameters were noted upon the fluorination of central thiophenes (**3**, Chart 1) [33]. Both SMDs displayed broad absorption with good thermal stability; however, the fluorinated analogue has comparatively deep HOMO energy level. The fluorination of the central unit induces better planarity in SMD **3** (dihedral angle of 0.52° between two thiophenes), than non-fluorinated SMD **2** and therefore gives rise to enhanced molecular packing and carrier mobility. Under optimized conditions, an inverted PV cell based on **3** gave a PCE ~ 7.14%. Liang *et al.* [34] designed and synthesized D2-A-D1-A-D2 type of SMs (**4a- e,** Chart 1) and systematically studied the effect of the number of thiophene units on the PCE of the fabricated device (**Table 1**). They concluded that the SMs with odd number of thiophene unit(s) have higher PCE compared to the ones having even number of thiophene units. Zhang *et al.* [35], designed and synthesized a new SMD **5** (Chart 1) composed of planar electron-withdrawing 1,3-bis(4-(2-ethylhexyl)-thiophen-2-yl)-5,7-bis(2-ethylhexyl) benzo[1,2-c:4,5-c′]-dithiophene-4,8-dione (BDD) unit as the central core. After thermal annealing (TA) and solvent vapor annealing (SVA), a PCE of 9.35% was achieved with high values of V_{oc}, J_{sc} and FF (Table 1). The high value of V_{oc} was attributed to the low HOMO energy level while the high J_{sc} and FF values were attributed to the enhanced absorption of blend films, fine-tuned morphology and good charge mobilities. These results suggest that using an electron-withdrawing central unit with a large planar structure and A–D–A configuration is an efficient way to achieve high performance PV cells. Hong *et al.* [36] designed and synthesized a new small molecule **6** (Chart 1), having dithieno[3,2- b:2′,3′- d]phosphole oxide (DTP) as the central core and 3-ethylrhodanine as termini separated by alkyl terthiophene. Since the DTP molecule forms an unusual hyperconjugation ring with rigid pyramidal geometry, which lowers the energy level of LUMO making them strong electron acceptor [37, 38]. The absorption spectrum of the SM **6** in solution and in thin film showed a broad absorption range (300 -750 nm) with maxima at 516 nm which was 78 nm red-shifted in thin film due to intermolecular π–π stacking (**Figure 3**). The SM **6** exhibited an emission peak at 724 nm which was significantly quenched (97%) in the **6**:$PC_{71}BM$ blend film (due to the polarizable nature of the DTP moiety and superior miscibility between **6** and $PC_{71}BM$). The BHJ device based on **6** exhibited a PCE value of 5.04% with a J_{sc} of 12.98 mA cm^{-2}, a V_{oc} of 0.79 V. These promising PCE values were

achieved without any pre- or post-treatments and were suggested that DTP-based small molecule can be a promising candidate for PV application.

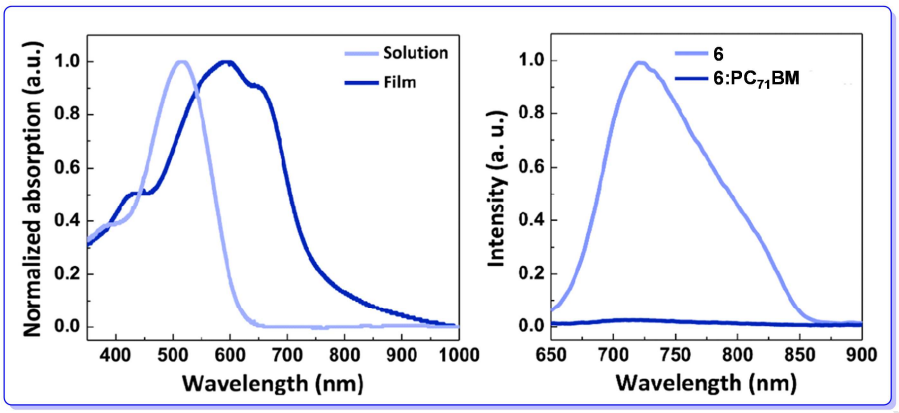

Figure 3: (a) Normalized UV–vis–NIR absorption spectra of **6** in $CHCl_3$ solution or as a thin film; (b) PL spectra of pure **6** and **6**:$PC_{71}BM$ blend films. Reproduced with the permission of Ref. [36].

Chen and co-workers [39] accessed BHJ-SCs based on *cis*-stilbene with or without a spiro linker, terthiophene arms and acceptor end groups **7(a-c)** (Chart 1). They reported that BHJ composed of spiro-containing molecule **7a** showed better light-harvesting ability than **7b**. The device based on the **7a** and $PC_{71}BM$ with 1,8-diiodooctane (DIO) additive exhibited more uniform and optimal domains with better percolation length in the film leading to PCE of 4.87% and a high FF of 64.1%. Along similar line Wang et al, [40] designed and synthesized three A-π-D-π-A SM **8** with spiro[cyclopenta[1,2-b:5,4-b′]dithiophene-4,9′-fluorene] (STF) as the central donor core. The SMs **8(a-c)** (Chart 1), showed wide absorption bands (300–850 nm) with high molar absorption coefficients (4.82×10^4 to 7.56×10^4 M^{-1} cm^{-1}) and relatively low HOMO levels (−5.15 to −5.38 eV). The optimized OSCs based on these molecules deliver PCEs of 6.68%, 3.30%, and 4.33% for **8a**, **8b**, and **8c**, respectively. The higher PCE of **8a**-based OSCs was attributed to its better absorption ability, higher and balanced charge mobilities, and superior active layer morphology. In fact, this was the first example of developing the A-π-D-π-A type small molecules with a spiro-central donor core for high-performance OSC applications.

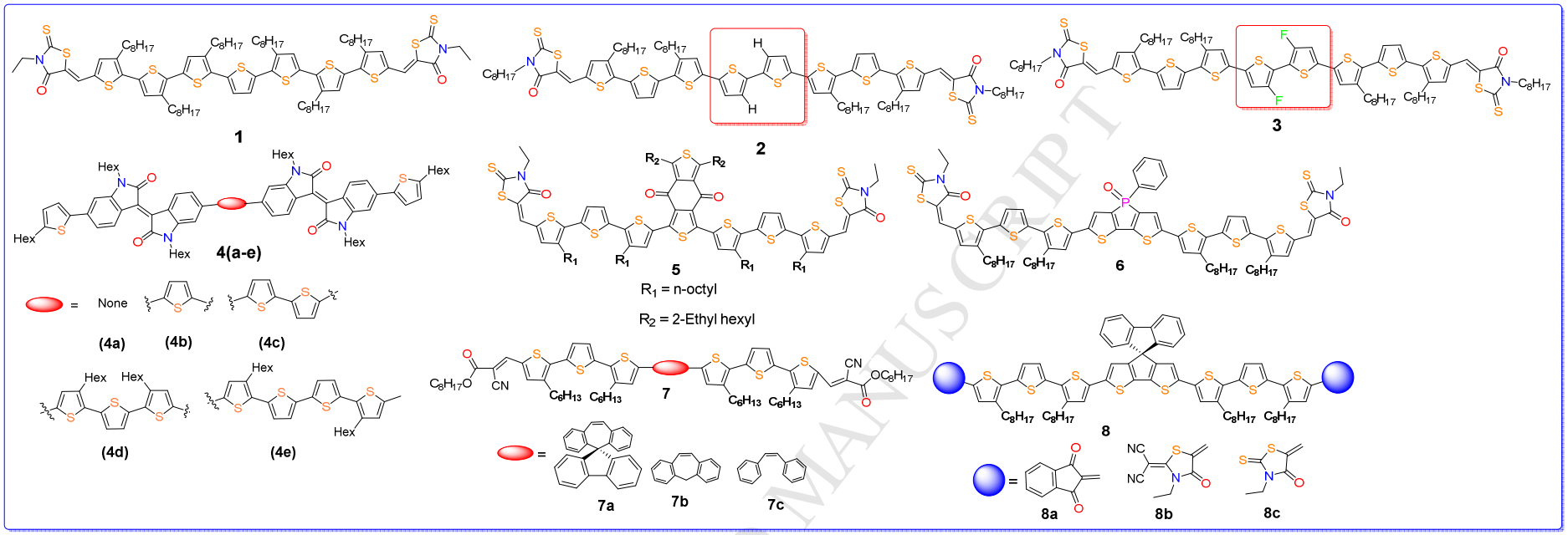

Chart 1: Oligothiophene-based SMDMs.

Table 1: Summary of frontier energy levels, device structure and performance parameters of oligothiophene-based SMDMs.

Entry	HOMO/ LUMO (eV)	Device architecture	V_{OC} (V)	J_{sc} (mA/cm^2)	FF (%)	PCE (%)	Ref.
1	−5.00/−3.28	ITO/PEDOT:PSS/**1**:$PC_{61}BM$/LiF/Al	0.92	13.98	47.4	6.10	[32]
2	–5.18/–2.68	ITO/PEDOT:PSS/**2**:$PC_{71}BM$/LiF/Al	0.86	10.26	66.8	5.89	[33]
3	–5.28/–2.80	ITO/PEDOT:PSS/**3**:$PC_{71}BM$/LiF/Al	0.93	11.03	69.6	7.14	[33]
4a	–5.52/–3.23	ITO/PEDOT:PSS/**4a**/Ca/Al	0.62	1.37	48.2	0.41	[34]
4b	–5.24/–3.61	ITO/PEDOT:PSS/**4b**/Ca/Al	0.82	5.32	49.2	2.16	[34]
4c	–5.32/–3.63	ITO/PEDOT:PSS/**4c**/Ca/Al	0.83	4.00	50.9	1.69	[34]
4d	–5.22/–3.69	ITO/PEDOT:PSS/**4d**/Ca/Al	0.78	6.59	46.9	2.40	[34]
4e	–5.16/–3.57	ITO/PEDOT:PSS/**4e**/Ca/Al	0.76	3.63	57.0	1.57	[34]
5	−5.12/−3.19	Glass/ITO/PEDOT:PSS/**5** /PrC60MA/Al	0.96	14.59	66.0	9.23	[35]
6	−5.10/−3.45	Glass/ITO/MoO_3/**6**:$PC_{71}BM$)/LiF/Al	0.79	12.98	49.0	5.04	[36]
7a	−5.38/−3.32	Glass/ITO/PEDOT:PSS/**7a:**$PC_{61}BM$/Al	0.97	7.93	64.1	4.87	[39]
7b	−5.25/−3.25	Glass/ITO/PEDOT:PSS/**7b:**$PC_{61}BM$/Al	0.90	1.36	32.7	0.39	[39]
7c	−5.31/−3.43	Glass/ITO/PEDOT:PSS/**7c:**$PC_{61}BM$/Al	1.00	1.50	27.5	0.41	[39]
8a	−5.38/−3.71	ITO/PEDOT:PSS/**8a**:$PC_{71}BM$/PDINO/Al	0.79	12.88	65.8	6.68	[40]
8b	−5.25/−3.61	ITO/PEDOT:PSS/**8b**:$PC_{71}BM$/PDINO/Al	0.88	10.08	48.9	4.33	[40]
8c	−5.15/−3.68	ITO/PEDOT:PSS/**8c**:$PC_{71}BM$/PDINO/Al	0.87	7.21	52.5	3.30	[40]

PEDOT:PSS = poly(3,4-ethylenedioxythiophene):polystyrene sulfonate, PDINO = perylenediimide *N*-oxide,

3.2. Oligothiophene-Benzodithiophene (BDT) Hybrids as SMDMs

In addition to thiophene and oligothiophenes based SMDMs, several benzodithiophene (BDT) based hybrid materials have been investigated recently (Chart 2). Table 2 shows the performance of OPV based on BDT hybrids. When fluorinated 2,2'-bithiophene unit was replaced by BDT and 3-ethylrhodanine by cyano functionalities, the resulting SM **9** (Chart 2) generated a PCE of 4.56% in combination of $PC_{61}BM$ as acceptor [41]. Interestingly, when 3-ethylrhodanine was installed back on SM **10** (Chart 2), it led to a sharp increase in PCE (6.38%) and significant rise in current density (J_{sc} = 10.78 mA cm^{-2}). The enhanced performance was attributed to the better light absorption of **10** compared to **9** [41]. Furthermore, when the acceptor was changed to $PC_{71}BM$, device based on **9** gave a significantly low efficiency as well as current density (PCE = 2.09%, J_{sc} = 3.74 mA cm^{-2}) while device based on **10** yielded an improved PCE (6.92%) and J_{sc} (11.40 mA cm^{-2}). All these PV parameters reached maximum values (PCE = 7.38%, V_{oc} = 0.93 V, J_{sc} = 12.21 mA/cm^2) by the addition of trimethylsiloxyl terminated polydimethylsiloxane (PDMs) during the film-forming process. These results clearly show that not only the acceptor but other additives also impact the performance of the device. Studies showed that the replacement of alkoxy group over BDT by alkyl [42] and thioether [43] also improves the device performance. For example, using oligomer **11** (Chart 2), PCE of about 8.26% was reported, while **12** (Chart 2) based device gave a maximum PCE of 9.95% [42, 43]. It is to be noted that the enhanced performance could not be attributed to the structure modification only but the morphology, absorption profile and structure of the active layer were also modified. The introduction of an extra alkylthio-thiophene as side chains on the BDT unit (**13,** Chart 2) resulted a PCE of 9.20% without any processing [44]. Interestingly, **13:**$PC_{71}BM$ based device with active area of 14.4 cm^2 generated PCE of 6.68%. A slight increase in performance (annealing dependent) was reported for devices based on donor **14** (9.6%) [45] and **15** (9.3%) [46] **(**Chart 3**)** bearing more branched side chains. Not only this, **14**-based device also afforded high fill factor (FF~70%) and PCE (~8%) at the active layer thicknesses up to 400 nm.

In order to commercialize OSCs, the successful demonstration of PV devices via printing method is essential to apply them into the roll-to-roll process. To verify the effect of the roll-to-roll compatible approach, Heo *et al.* [47] used small molecule **15** and fabricated three types of devices: (a) as cast films without any treatment, (b) blend films following the SVA treatment and (c) blend films processed with a diphenyl ether (DPE) additive slot-die printed devices with a normal structure of ITO/PEDOT:PSS/**15**:$PC_{71}BM$/Ca/Al. The device (a) without any treatment showed PCE of 3.81%. The device (b) showed enhanced PCE of 7.46%, as reported earlier [46]. Interestingly, DPE processed devices also exhibited high PCE (6.56%), due to a significant increase in FF and J_{sc}, even though there were slight

drops in open-circuit voltage (V_{oc}). Furthermore, authors also achieved a PCE of 4.80% using large-area (10 cm^2) PV modules (Figure 4). These results showed signifies the potential of SMDMs in the industrial-scale production of OSCs via roll-to-roll compatible printing methods without using halogenated solvent.

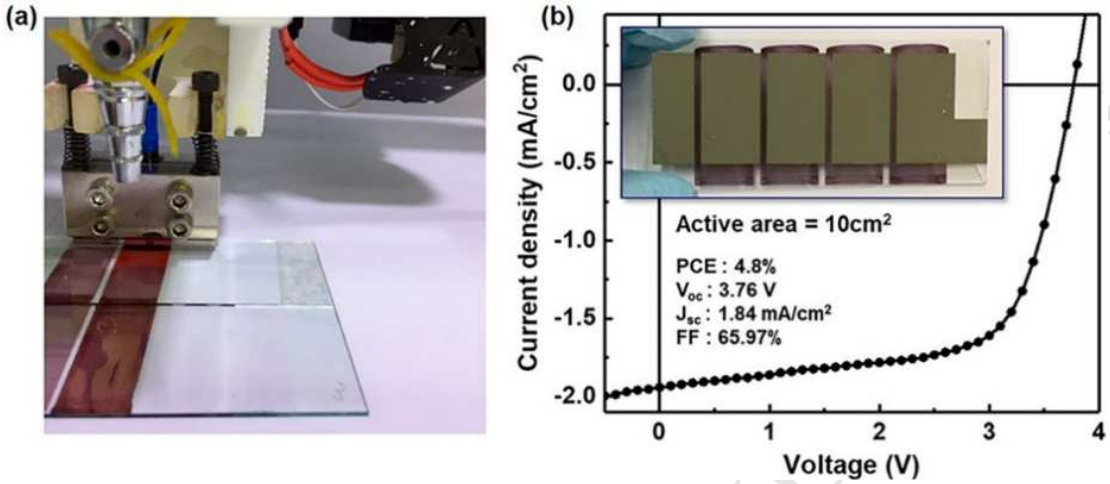

Figure 4: (a) Photographic image of slot-die-coated large area photovoltaic modules during printing process and (b) corresponding J-V curves cells based on **15**. Reproduced with the permission of Ref. [47].

Badgujar et al. [48] synthesized (**16** and **17,** Chart 2) and conducted a comparative study of the device performance by increasing the number of BDT units in the SMD core and studied how the number of BDT units influences the PV performance. They found that the presence of extra BDT units in **17** gives rise to strong intermolecular interaction, which promoted the desired interconnected structure and therefore, enhanced exciton diffusion and free-charge-carrier transport as compared to **16**. The device based on **17** shows PCE of 8.56% with a high FF of 73% under AM 1.5 G irradiation (100 mW cm^{-2}). Since this PCE is achieved without any additive, the result is unambiguously important for high reproducibility and fabrication of large-area modules. The performance of the device based on **17** with an area of 777.5 cm^2 showed PCE of 7.45% compared to 4.5% as shown by **16 (**Fig. 5a)**.** In similar aspect, Guo et al, [49] designed and synthesized two unsymmetrical BDT core monomer **18** and dimer **19** (Chart 2). The dimer was connected by octamethylene spacer. The device based on monomer **18** showed a PCE higher (8.18%) compared to the dimer **19 (**7.07%). The lower PCE of the dimer was blamed to lower J_{sc} (10.88 mA cm^{-2}), which in turn related to the poor absorption profile (Fig. 5b), low internal quantum efficiency and photo-induced charge transfer in the dimer.

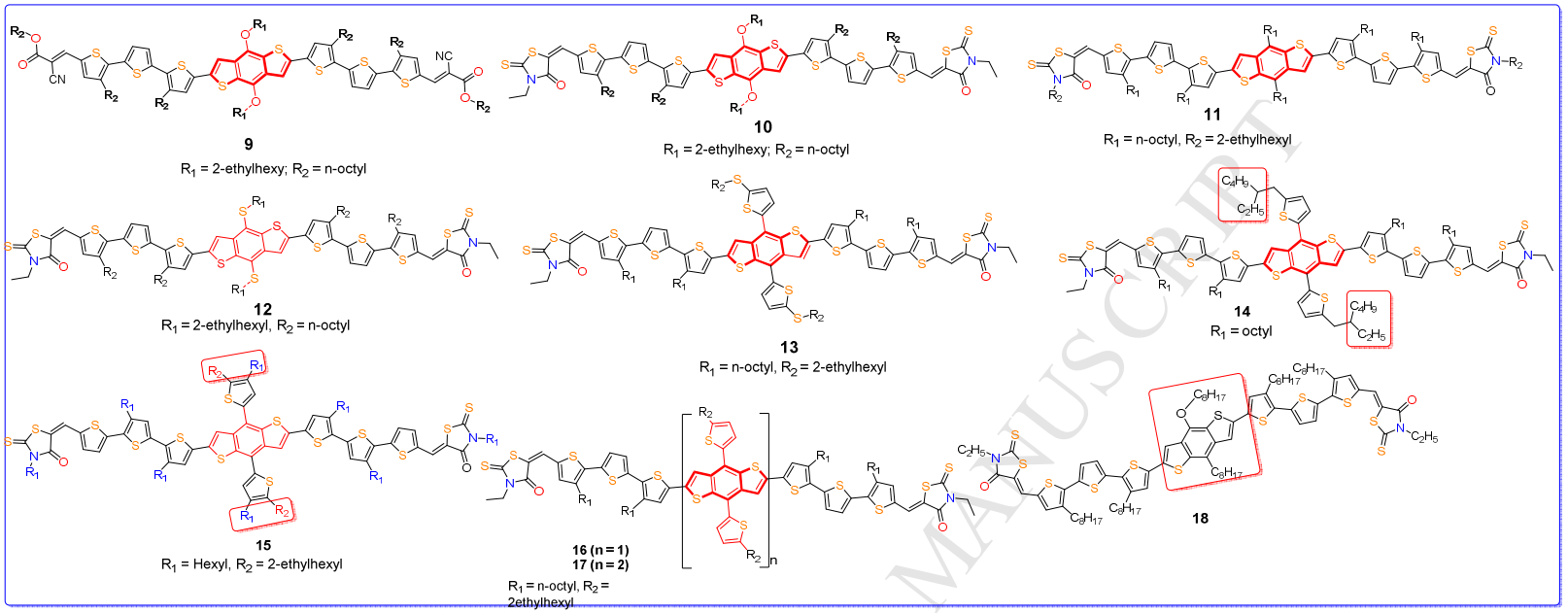

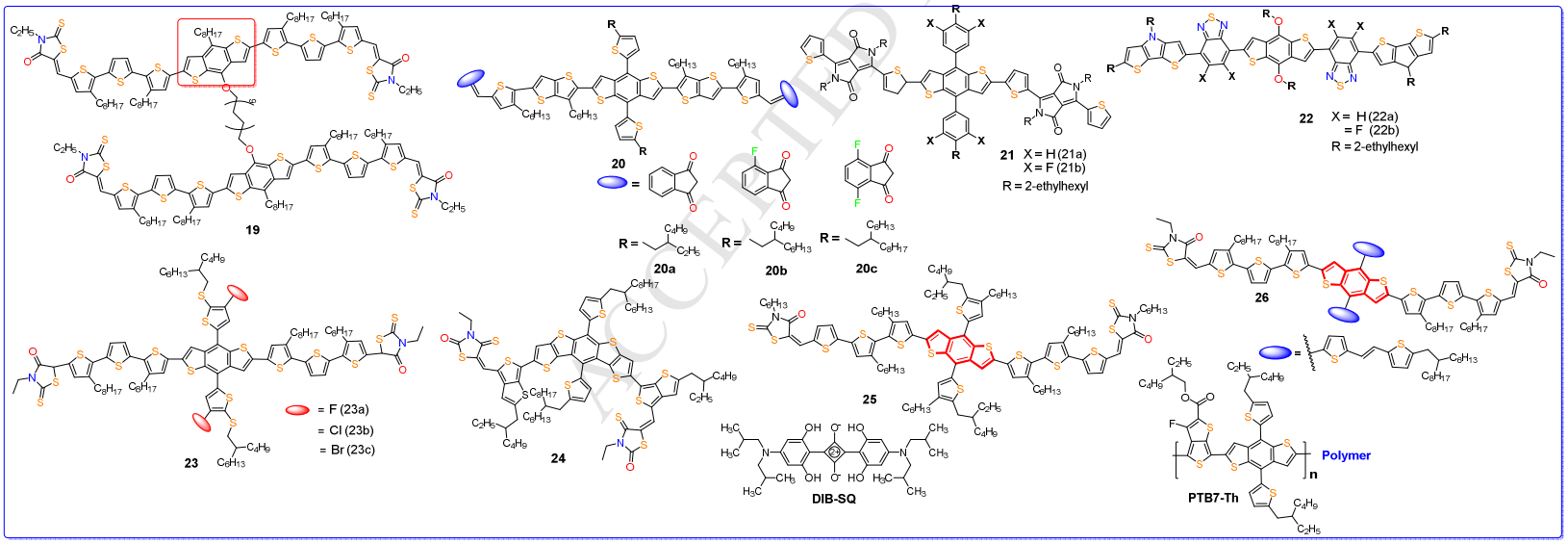

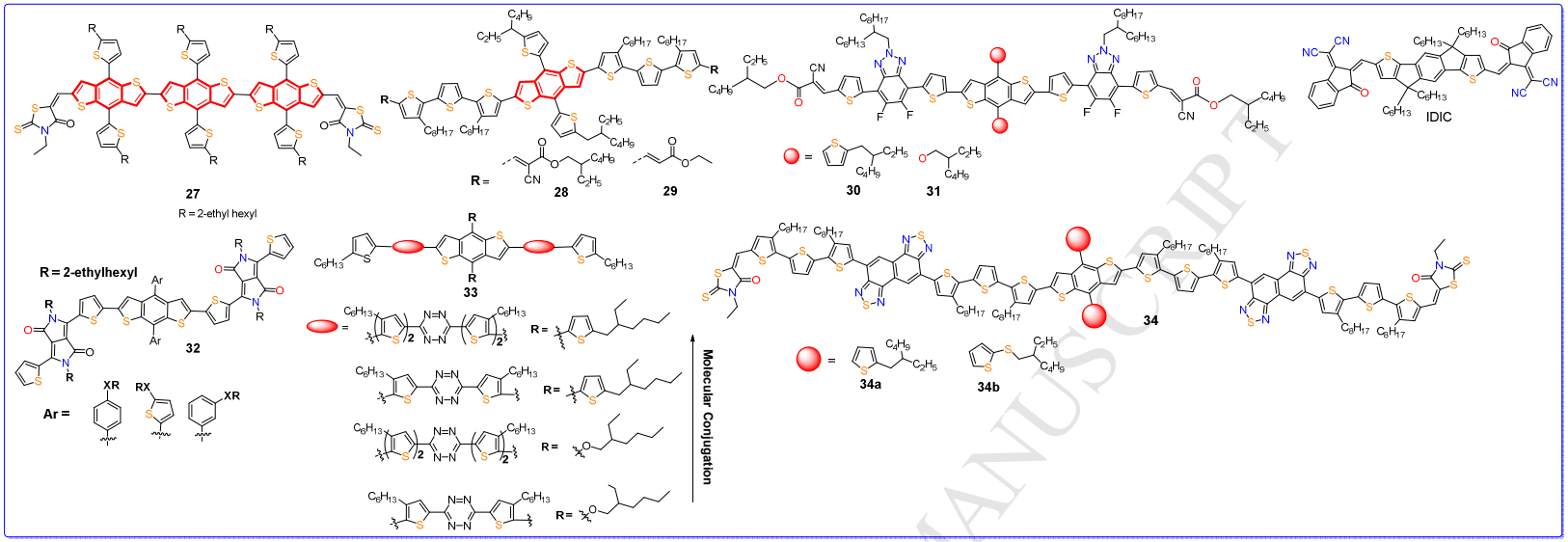

Chart 2: Chemical structures of benzodithiophene (BDT) hybrids used as SMDMs.

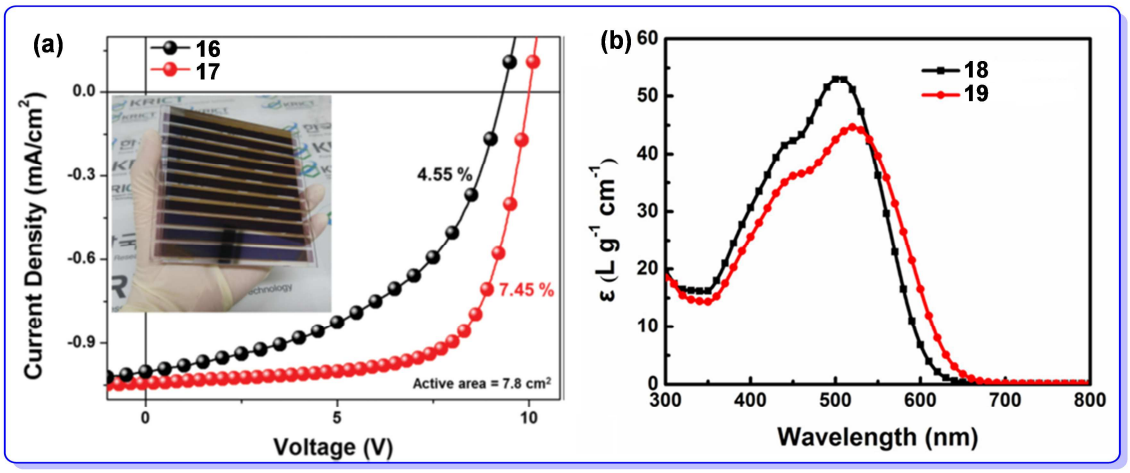

Figure 5: (a) Characteristic *J* – *V* curves for the optimized **16**: $PC_{71}BM$ and **17**:$PC_{71}BM$ large, rigid-module devices (777.5 cm ^{2}) under simulated AM 1.5 G irradiation (b) UV–vis absorption spectra of **18** and **19** in dilute chloroform solutions. Reproduced with the permission of Refs. [48] and [49].

In another very interesting study Deng et al. [10], combined a traditional molecular design with fluorination. They designed and synthesized three SMDs **(20a-e**, Chart 2**)** with increasing number of fluorine atoms, **20a**, **20b** and **20c**. The designed molecules showed optimal morphology which is important for charge transfer, charge collection and recombination suppression leading to reduced loss of V_{oc}, J_{sc} and FF simultaneously. As a consequence, fluorinated molecules exhibited excellent inverted device performance, and an average PCE of 11.08% and FF 76.0% was achieved with **20c** having two fluorine atoms. With very similar strategy, Eastham *et al.* [50] designed two new small molecule based on diketopyrrolopyrrole–benzodithiophene–diketopyrrolopyrrole (BDT-DPP_2) skeleton with and without fluorine on the aromatic side chains **21a** and **21b** (Chart 2). The ternary SC with varying ratios of two SMDs and $PC_{61}BM$ resulted in tunable V_{oc} (0.833-0.944 V) due to a fluorination-induced shift in energy levels and the electronic "alloy" formed from the miscibility of the two SMDs. A 15% increase in PCE is observed at the optimal ternary SMD ratio, with significantly increased J_{sc} (9.18 mA/cm^2), due to the increased optical absorption of the blend. Busireddy *et al.* [51] designed and studied the effect of fluorination on PV performances of two small D_1–A–D_2–A–D_1 type skeleton having 2,4-bis(2-ethylhexyl)-4*H*-dithieno[3,2-*b*:2′,3′-*d*]pyrrole (EHDTP, D_1) and 4,8-bis((2-ethylhexyl)oxy) benzo[1,2-*b*:4,5-*b*′]dithiophene (OBDT, D_2) as the terminal and central donor, and benzo[*c*][1,2,5] thiadiazole (**22a**) and 5,6-difluorobenzo[*c*][1,2,5]thiadiazole (**22b**) (Chart 2**)**. The fabricated BHJ-SCs with two-step annealed (thermal followed by SVA) active layers of **22a** and **22b**, show overall PCE of 5.46% and 7.91%, respectively. The superior performance of the **22b** based device was accheived to the favorable morphology and nanoscale interpenetrating network in the **22b**:$PC_{71}BM$ active layer. This was induced by the fluorine atoms on the BT acceptor, which significantly enhances

the dissociation of excitons, charge transport and the charge collection efficiency, and suppressed bimolecular recombination in the BHJ. The observed higher PCE indicated **22b** is one of the best BT based donor materials for small molecular BHJ-SCs.

Ji et al. [52] investigated the effect of molecular structure i.e., halogenation on the properties and consequently on the PV performance. They reported three new SMs (**23 a-c**, Chart 2) incorporating BDT central core having different halogen atoms (fluorine, chlorine and bromine) and 3-ethylrhodanine as the terminal groups. Due to the presence of fluorine atom in SMD, film composed of **23a**:$PC_{71}BM$ showed a high degree of crystallinity and poor phase of blend film. Replacing fluorine by chlorine (**23b**) and bromine (**23c**) led to decreased crystallinity; however, strong aggregations were effectively suppressed. The fabricated device with the Cl-bearing SM (**23b**) exhibited the best PCE value of 10.78 % (**Figure 6**), V_{oc} of 0.96 eV, a J_{sc} of 14.92 mA cm^{-2} and a FF of 75.3%. To reveal the structure–property relationship of the aromatic side-chain in substituted IDT-based SMDMs as a function of π-bridge and the post annealing conditions, Liu et al. [53] reported a molecule **24** (Chart 2) which showed a PCE of 8.17%, V_{oc} of 0.904 V, J_{sc} of 13.33 mA cm^{-2}, and a FF of 67% after solvent annealing (SVA)

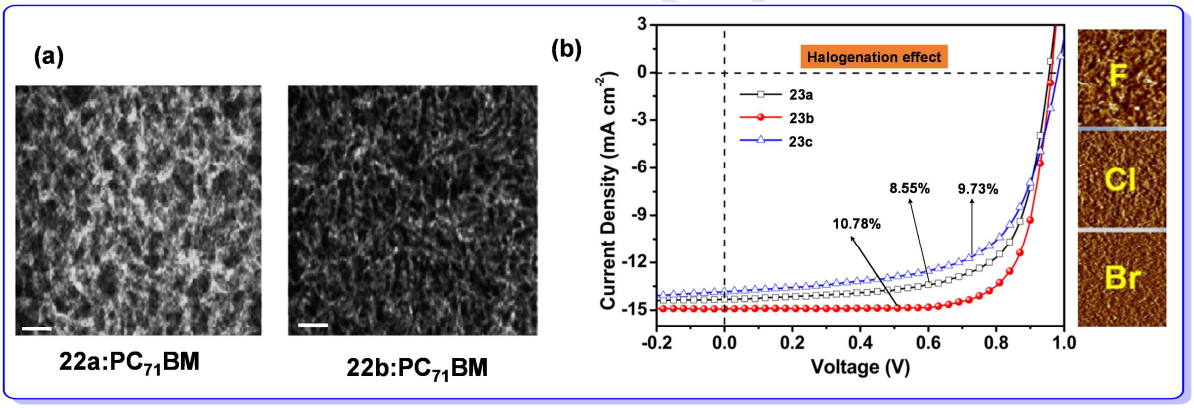

Figure 6: Transmission electron microscopy (TEM) images of TSA treated **22a**:$PC_{71}BM$ and **22b**:$PC_{71}BM$ thin films; bar is 100 nm and (b) Optimized J-V curves for the SM-OSCs based on **23a-c**. Reproduced with the permission of Refs. [51] and [52].

The fabrication of ternary OSCs have attracted much interest [54-56] due to the absorption range without the use of complicated tandem cell structures. In this context, Zhang *et al.* [57] fabricated OSCs based on small molecule (**25**, Chart 2), **25**:$PC_{71}BM$, which shows PCE of **9.37%**. In order to fabricate a ternary OSC (**Figure 7a**), they used small organic molecule DIB-SQ (6 wt%) as the third component in the host **25**:$PC_{71}BM$. The fabricated device shows an incredibly high PCE of 10.3% and is approximately improved by 10% compared to the binary device. This enhancement in PCE is due to increased J_{SC} (15.44 $mAcm^{-2}$) and FF (73.8%), which is due the improved photon harvesting of active layer, enhanced energy transfer from **25** to DIB-SQ (**Figure 7b**) and molecular packing for efficient exciton dissociation and charge transport.

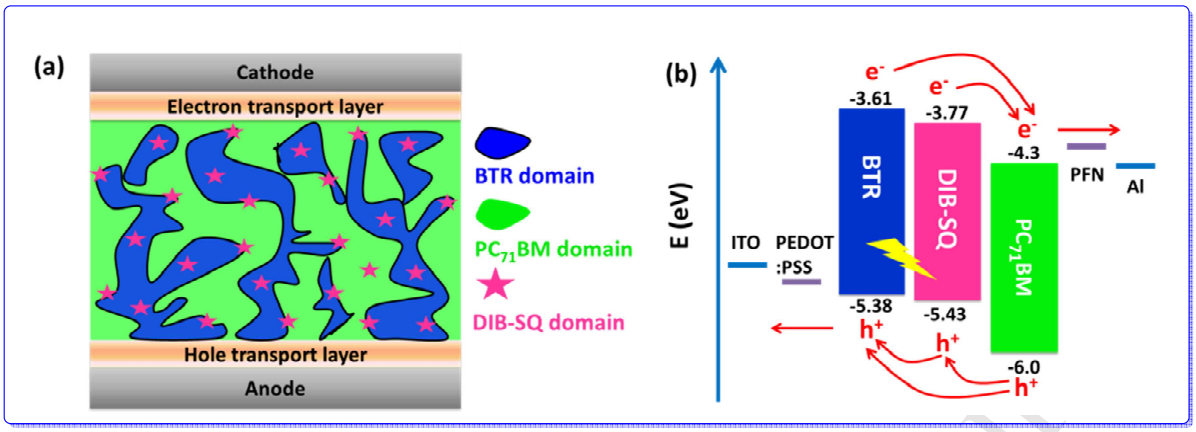

Figure 7: (a) Schematic diagram of ternary active layer; (b) Energy levels of used materials (arrows represent charge carrier transport direction and lightning bolt represents energy transfer from **25** to DIB-SQ). Reproduced with the permission of Ref. [57].

Similarly, Huang and co-workers, [58] fabricated another ternary OSC with the same nematic liquid crystalline SMDM **25** but different polymer donor i.e., **PTB7-Th:$PC_{71}BM$** (Chart 2). The introduction of **25** into the binary system improved the morphology of the blend film, decreased π–π stacking distance, enlarged coherence length, and enhanced domain purity. These modifications led to efficient charge separation, faster charge transport, and less bimolecular recombination, resulting into PCE of 11.40% even with thick active layer (250 nm).

Zhu *et al.* [59], designed and synthesized a **26** SM (Chart 2) and the binary device based on it showed a PCE of 5.71% with acceptor $PC_{71}BM$. Furthermore, ternary OSC fabricated by doping 10 wt% of **26** in **PTB7-Th:$PC_{71}BM$**, improved charge-mobility, reduced resistance and better phase separation. This ternary device showed a PCE of 7.77% with a V_{oc} 0.77 V, a J_{SC} 14.52 mA $cm^{-2}$and a FF of 70.3%. Yang *et al.* [60] have designed and synthesized a new wide band gap (WBG) small molecule **27** (Chart 2) by incorporating a two-dimensional trialkylthienyl-substituted on the BDT core, the resulting material has band gap (E_g^o) of 2.0 *eV* with a low-lying HOMO level of −5.51 eV. They further constructed a non-fullerene small-molecule organic solar cell (NFSM-OSC) by empolying IDIC as acceptor (Chart 2). The device showed 9.08% PCE with a high V_{oc} (0.98 V). This result demonstrates that the molecular design of a WBG donor to create a well-matched donor–acceptor pair with a low band gap (LBG) non-fullerene small-molecule acceptor with a subtle morphological control provides great potential to realize high-performance NFSM-OSCs.

In a similar effort, Qui et al. [61] designed and synthesized two WBG acceptor-donor-acceptor (A-D-A) SMs bearing electron-withdrawing ester end group with cyano (CN) group on ester **28** and SM without the cyano group **29** and used acceptor molecule LA-1 (Chart 2). The presence of cyano group on **28** gives the molecule a stronger absorption (ε = 8.78 × 10^4 M^{-1} cm^{-1} for **28** and 7.64 × 10^4 M^{-1} cm^{-1} for **29**), lower-lying HOMO energy level and higher

charge-mobility compared to the SM **29** which lacks cyano group. Film based on **28** and **29** exhibits maximum peak at 566 and 521 nm which is 66 and 55 nm red-shifted relative to its solution. The device with **28** shoeds PCE of 10.11% and a high FF of 73.55% compared to molecule **29**, which shows PCE of 5.32%. The results indicate that the cyano substitution in **28** plays an important role in improving the PV performance of the NFSM-OSC. Bin *et al.* [62] designed and synthesized medium bandgap SM **30** (Chart 2) with bithienyl-benzodithiophene (BDTT) as central donor unit and fluorobenzotriazole as acceptor unit. They further synthesized a control molecule **31** (Chart 2) without thiophene conjugated side chains on the BDT. The device based on **30** as donor and IDIC as acceptor shows a superior PCE 9.73% compared to device based on **31** with the same configuration. The superiority of **30** based device was attributed to intense absorption, low-lying HOMO energy level, higher hole mobility and ordered bimodal crystallite packing in the blend films. In addition to this a large area (10.0 cm^2) OSC based on **30**:IDIC demonstrated a relatively higher PCE upto **8.52**%. These results clearly attest that fluorobenzotriazole based 2D conjugated organic D-A molecules have a bright future for applications of NFSM-OSC.

Unlike the performance parameters V_{oc} and J_{sc}, optimization of the FF is not so clearly understood [29] to envision high PV performance from the OPV. In order to optimize the FF, Aldrich *et al.* [63] designed and synthesized a series of small molecules by incorporating the chalcogen (sulphur, oxygen and selenium) into the side chain **32** (Chart 2). It was noted that SM with higher atomic number (Z) chalcogen is shows a enhanced FF. The found significantly high FF ~8% FF and the increased was gained on moving from O to S to Se across the series of SMDs. This significant enhancement in the FF is due to the combination of more ordered morphology and decreased charge recombination in blend films for the high-Z chalcogen SMDs. Similarly Wang *et al.* [64] synthesized SM **33** (Chart 2), D2-A-D1-A-D2, where D1 an alkylthienyl substituted BDT unit, A represents a tetrazine (Tz) unit, and D2 is a bithiophene or terthiophene ending donor unit. The results of PV study showed that extension of main chain π-conjugation enhanced device performance (V_{oc} = 1.03 V and FF = 65.3% with PCE = 6.49%), while in the side chain leads to larger absorption coefficients, lower HUMO levels, and more favorable blend morphology.

Wan *et al.* [65] designed and synthesized two SMs **34a** and **34b** (Chart 2) with benzo[1,2-*b*:4,5-*b'*]dithiophene (BDT) as the central donor unit and electron-deficient naphtho[1,2-*c*:5,6-*c'*]bis[1,2,5]thiadiazole (NT) group. This extended the π-conjugation length of the whole small molecular backbone. The introduction of sulfur atom in the side chains further lowers the HOMO/LUMO levels and results in a higher V_{oc} of 0.93 V with a very low E_{loss} of 0.57 V for the **20** devices. Based on rational material design and device engineering, the resulting SM-OSCs processed with a halogen-free CS_2 solvent exhibited a high efficiency of **11.53%** with a very small energy loss of 0.57 eV.

Table 2: Summary of frontier energy levels, device structure and performance parameters of oligothiophene-Benzodithiophene (BDT) hybrids.

Entry	HOMO/ LUMO (eV)	Device architecture	V_{OC} (V)	J_{sc} (mA/cm^2)	FF (%)	PCE (%)	Ref.
9	–5.04/–3.24	Glass/ITO/PEDOT–PSS/**9**/LiF/Al	0.93	3.74	60.1	2.09	[41]
10	–5.02/–3.27	Glass/ITO/PEDOT–PSS/**10**/LiF/Al	0.93	12.21	65.0	7.38	[41]
11	–5.08/–3.27	ITO/(PEDOT-PSS)/**11**:$PC_{71}BM$/ZnO/Al	0.94	12.56	70.0	8.26	[42]
12	–5.07/–3.30	ITO/PEDOT:PSS/**12**:$PC_{71}BM$/ETL-1/Al	0.91	14.45	73.0	9.60	[43]
13	–5.18–3.25	ITO/PEDOT:PSS/**13**:$PC_{71}BM$/Ca/Al	0.97	13.45	70.5	9.20	[44]
16	–5.14/–3.37	ITO/PEDOT:PSS/**16**: $PC_{71}BM$ /Ca/Al	0.89	13.02	62.0	7.18	[48]
17	–5.13/–3.37	ITO/PEDOT:PSS/**17**: $PC_{71}BM$ /Ca/Al	0.89	13.17	73.0	8.56	[48]
18	–4.94/–3.30	ITO/PSS:PEDOT/**18**:$PC_{71}BM$/ETL-1/Al	0.87	12.54	74.0	8.18	[49]
19	–5.02/–3.30	ITO/PSS:PEDOT/**19**:$PC_{71}BM$/ETL-1/Al	0.86	10.62	72.0	7.07	[49]
20a	–4.91/–3.20	ITO/ZnO/**20a**/MoO_x/Ag	0.93	14.0	64.0	8.3	[10]
20b	–4.98/–3.28	ITO/ZnO/**20b**/MoO_x/Ag	0.94	15.3	72.0	10.4	[10]
20c	–5.05/–3.37	ITO/ZnO/**20c**/MoO_x/Ag	0.95	15.7	76.0	11.3	[10]
21a	–5.36/–3.66	ITO/PEDOT:PSS/**21a**: $PC_{71}BM$ /LiF/Al	0.83	8.36	59.6	4.15	[50]
21b	–5.47/–3.75	ITO/PEDOT:PSS/**21b**: $PC_{71}BM$ /LiF/Al	0.94	7.81	57.8	4.26	[50]
22a	–5.55/–3.65	ITO/PEDOT:PSS/**22a**: $PC_{71}BM$/PFN/Al	0.91	10.52	57.0	5.46	[51]
22b	–5.66/–3.69	ITO/PEDOT:PSS/**22b**: $PC_{71}BM$/PFN/Al	0.98	12.23	66.0	7.91	[51]
23a	−5.05/−2.88	ITO/PEDOT:PSS/**23a**: $PC_{71}BM$ /Ca/Al	0.95	14.31	68.9	9.37	[52]
23b	−5.06/−2.88	ITO/PEDOT:PSS/**23b**: $PC_{71}BM$ /Ca/Al	0.96	14.92	75.3	10.78	[52]
23c	−5.06/−2.89	ITO/PEDOT:PSS/**23c**: $PC_{71}BM$ /Ca/Al	0.98	13.85	63.1	8.55	[52]
24	−5.06/−3.45	ITO/PEDOT:PSS/**24**:$PC_{71}BM$/Ca/Al	0.90	13.33	67.0	8.17	[53]
25	−5.38/−3.61	Ternary	0.90	15.44	73.8	10.3	[57]
25	−5.38/−3.61	Ternary	0.75	21.4	70.0	11.40	[58]
26	−5.29/−3.27	Ternary	0.77	14.52	70.3	7.77	[59]
27	−5.29/−3.34	ITO/MoO_3/**27**:IC-C6IDT-IC/Al	0.98	14.25	65.0	9.08	[60]
28	−5.24/−2.82	ITO/PEDOT:PSS/**28**:IDIC/PDINO/Al	0.90	15.18	73.55	10.11	[61]
29	−5.04/−2.70	ITO/PEDOT:PSS/**29**:IDIC/PDINO/Al	0.76	10.77	64.40	5.32	[61]
30	−5.31/−3.03	ITO/PEDOT:PSS/**30**:IDIC:PDINO/Al	0.977	15.21	65.46	9.73	[62]
31	−5.28/−3.01	ITO/PEDOT:PSS/**31**:IDIC:PDINO/Al	0.955	10.51	54.89	5.51	[62]

PEDOT:PSS = poly(3,4-ethylenedioxythiophene):polystyrene sulfonate, PDINO = perylenediimide *N*-oxide, PFN = poly(9,9-bis(3′-(*N*,*N*-dimethylamino)propyl)fluorene-2,7-diyl)-*alt*-(9,9-dioctylfluorene-2,7-diyl).

3.3. Indacenodithiophene (IDT)-based SMDMs

Indacenodithiophene (IDT) is another intriguing class of fragment known for its strong PV potential. Table 3 summarizes the performance of devices based on IDT. Wang et al. [66] reported two tetrafluorinated new SMs **35** and **36** (**Chart 3**), consist of electron-rich central core (IDT) and electron-deficient difluorobenzothiadiazole as acceptor units and donor end-capping groups having different π-bridge (thiophene and selenophene). The π-bridge and central core units in these small molecules played an important role in the formation of the nanoscale separation of the blend films. The presence of the electron-rich selenophene spacer in the molecule **36** has prominent effect on the absorption spectrum and molar extinction coefficient which shows a red shift of 20 nm compared to molecule **35** (554 nm). The device based on selenophene spacer i.e., **36**, showed superior PCE (7.31%) with FF ~ ~70% compared to **35** (PCE 5.73% and FF ~ 58%) after post annealing treatments due to the optimized morphology and improved charge transport.

With the similar strategy of using the electron-rich selenium, Wang *et al.* [67] have designed two mixed sulphur and selenium based small molecules **37a** and **37b** (Chart 3), with the selenium and sulphur atoms in different positions. Interestingly, the BHJ-OSC device based on molecule **37b** showed a PCE of 9.3%, which is the highest efficiency based on donor end-capped oligomers. These results clearly demonstrate that a sequence of π-bridge and annealing treatments play important roles for improving ordered and crystalline morphology and enhanced PCE, and therefore can provide useful strategy toward highly efficient SMD for BHJ-OSCs.

The SM-OSCs have received considerable attention; however, a key factor which limits the performance of these small molecules is their large energy loss (E_{loss} 0.6 and 1.0 eV) compared to perovskite and inorganic SCs (E_{loss} < 0.5 eV). In this aspect, Yang *et al.* [68] designed a new A-D-A type dimeric squarine small donor molecule **38** (Chart 3). The solution of the molecule showed strong absorption which stretches in the NIR region (600 – 750 nm) with a maximum molar extinction coefficient of 2.84×10^5 M^{-1} cm^{-1} at 705 nm due to effective delocalization of the π-electron between their constituent units. The BHJ device fabricated by this low band-gap materials (E_g^o = 1.49 eV) exhibited high V_{oc} (0.93 V), high PCE (7.05%) and low E_{loss} (0.56 eV), which is the first report wherein SM-OSCs result in such a low E_{loss}, while simultaneously exhibiting a considerably high V_{oc} and an excellent PCE. The result suggests that the A–D–A-structured dimeric molecular strategy can be used as an effective way to obtain low E_{loss} and high V_{oc}, thereby achieving improved performance.

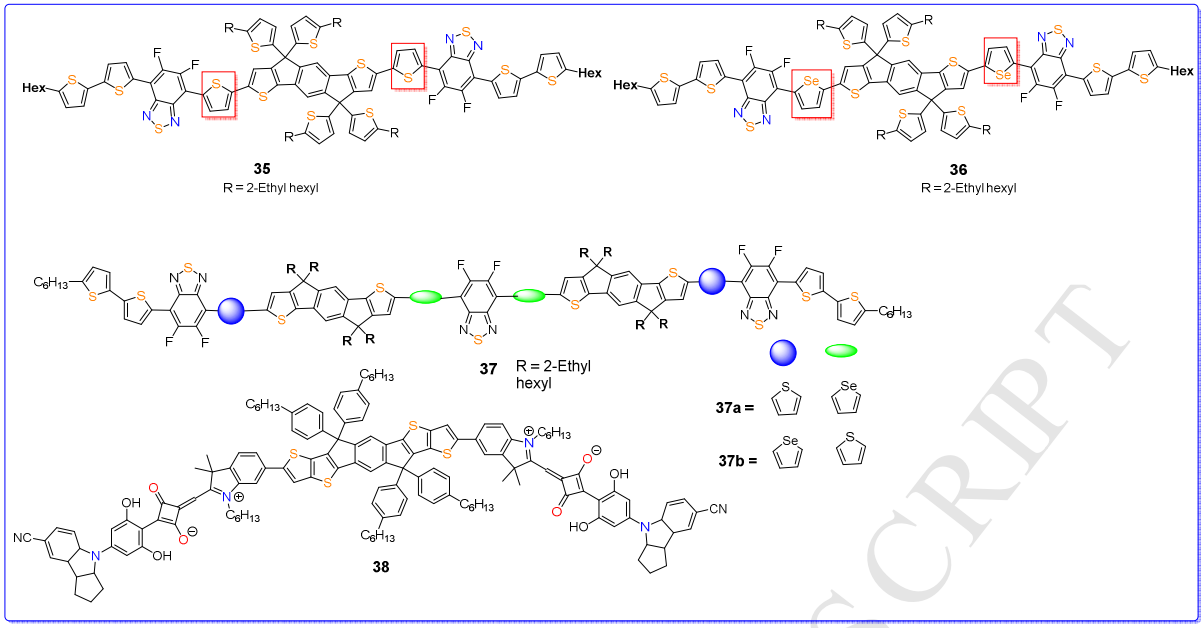

Chart 3: Chemical structures of Indacenodithiophene (IDT)-based SMDMs.

Table 3: Summary of frontier energy levels, device structure and performance parameters of the Indacenodithiophene (IDT)-based SMDMs.

Entry	HOMO/ LUMO (eV)	Device architecture	V_{OC} (V)	J_{sc} (mA/cm^2)	FF (%)	PCE (%)	Ref.
35	−5.43/−3.65	ITO/PEDOT:PSS/**35**:$PC_{71}BM$/PFN/Al	0.85	11.17	58.0	5.45	[66]
36	−5.41/−3.67	ITO/PEDOT:PSS/**36**:$PC_{71}BM$/PFN/Al	0.82	12.62	69.0	7.16	[66]
37a	−5.24/−3.19	ITO/PEDOT:PSS/**37a**:**$PC_{71}BM$**/PFN/Al	0.85	11.23	67.0	6.44	[67]
37b	−5.28/−3.22	ITO/PEDOT:PSS/**37b**:**$PC_{71}BM$**/PFN/Al	0.87	14.30	72.0	9.26	[67]

PEDOT:PSS = poly(3,4-ethylenedioxythiophene):polystyrene sulfonate, PFN = poly(9,9-bis(3′-(*N*,*N*-dimethylamino)propyl)fluorene-2,7-diyl)-*alt*-(9,9-dioctylfluorene-2,7-diyl).

4. Conclusion and future outlook

During the last three years, the active materials for OPV have grown enormously in PCE and broke the threshold (10%) for potential commercial viability. The progress in the design of small organic donor molecule has slowed down a bit; nevertheless, it is promising. The challenges of preventing recombination, absorbing more broadly and strongly in the visible to near-infrared part of the solar spectrum, and optimizing morphological characteristics to facilitate charge transport still remain. But the steady ongoing progress made towards overcoming these obstacles coupled with the easy tunability and versatility of small organic molecule based donor materials point to a bright future for their continued success as solar energy materials.

Acknowledgements

MSK thanks His Majesty's Trust Fund for Strategic Research (Grant No. SR/SQU/SCI/CHEM/16/02) for funding. MSK also acknowledges The Research Council (TRC), Oman and HM's Trust Fund, Oman for post-doctoral fellowships to RI and AH, respectively.

Refrences

[1] P.-L. Ong, I. Levitsky, Organic / IV, III-V Semiconductor Hybrid Solar Cells, Energies, 3 (2010) 313.

[2] D.M. Powell, M.T. Winkler, H.J. Choi, C.B. Simmons, D.B. Needleman, T. Buonassisi, Crystalline silicon photovoltaics: a cost analysis framework for determining technology pathways to reach baseload electricity costs, Energy & Environmental Science, 5 (2012) 5874-5883.

[3] C.A. Wolden, J. Kurtin, J.B. Baxter, I. Repins, S.E. Shaheen, J.T. Torvik, A.A. Rockett, V.M. Fthenakis, E.S. Aydil, Photovoltaic manufacturing: Present status, future prospects, and research needs, Journal of Vacuum Science & Technology A: Vacuum, Surfaces, and Films, 29 (2011) 030801.

[4] Y. Okamoto, W. Brenner, Organic semiconductors, Reinhold Pub. Corp.1964.

[5] M.A. Green, K. Emery, Y. Hishikawa, W. Warta, E.D. Dunlop, D.H. Levi, A.W.Y. Ho-Baillie, Solar cell efficiency tables (version 49), Progress in Photovoltaics: Research and Applications, 25 (2017) 3-13.

[6] M.C. Scharber, D. Mühlbacher, M. Koppe, P. Denk, C. Waldauf, A.J. Heeger, C.J. Brabec, Design Rules for Donors in Bulk-Heterojunction Solar Cells—Towards 10 % Energy-Conversion Efficiency, Adv. Mater., 18 (2006) 789-794.

[7] C.W. Tang, A.C. Albrecht, Photovoltaic effects of metal–chlorophyll-a–metal sandwich cells, The Journal of chemical physics, 62 (1975) 2139-2149.

[8] C.W. Tang, Two-layer organic photovoltaic cell, Appl. Phys. Lett., 48 (1986) 183-185.

[9] L. Yang, S. Zhang, C. He, J. Zhang, H. Yao, Y. Yang, Y. Zhang, W. Zhao, J. Hou, New Wide Band Gap Donor for Efficient Fullerene-Free All-Small-Molecule Organic Solar Cells, J Am Chem Soc, 139 (2017) 1958-1966.

[10] D. Deng, Y. Zhang, J. Zhang, Z. Wang, L. Zhu, J. Fang, B. Xia, Z. Wang, K. Lu, W. Ma, Z. Wei, Fluorination-enabled optimal morphology leads to over 11% efficiency for inverted small-molecule organic solar cells, 7 (2016) 13740.

[11] W. Zhao, S. Li, H. Yao, S. Zhang, Y. Zhang, B. Yang, J. Hou, Molecular Optimization Enables over 13% Efficiency in Organic Solar Cells, J. Am. Chem. Soc., 139 (2017) 7148-7151.

[12] A. Salleo, R.J. Kline, D.M. DeLongchamp, M.L. Chabinyc, Microstructural characterization and charge transport in thin films of conjugated polymers, Adv. Mater., 22 (2010) 3812-3838.

[13] T.D. Anthopoulos, B. Singh, N. Marjanovic, N.S. Sariciftci, A.M. Ramil, H. Sitter, M. Colle, D.M. de Leeuw, High performance n-channel organic field-effect transistors and ring oscillators based on C-60 fullerene films, Appl. Phys. Lett., 89 (2006) 213504.

[14] D.J. Gundlach, K.P. Pernstich, G. Wilckens, M. Gruter, S. Haas, B. Batlogg, High mobility n-channel organic thin-film transistors and complementary inverters, J. Appl. Phys., 98 (2005) 064502.

[15] J. Roncali, Molecular Bulk Heterojunctions: An Emerging Approach to Organic Solar Cells, Acc. Chem. Res., 42 (2009) 1719-1730.

[16] T. Ameri, G. Dennler, C. Lungenschmied, C.J. Brabec, Organic tandem solar cells: A review, Energy & Environmental Science, 2 (2009) 347-363.

[17] K.A. Mazzio, C.K. Luscombe, The future of organic photovoltaics, Chem. Soc. Rev., 44 (2015) 78-90.

[18] M.S. Khan, M.K. Al-Suti, J. Maharaja, A. Haque, R. Al-Balushi, P.R. Raithby, Conjugated poly-ynes and poly(metalla-ynes) incorporating thiophene-based spacers for solar cell (SC) applications, J. Organomet. Chem., 812 (2016) 13-33.

[19] O. Ostroverkhova, Organic Optoelectronic Materials: Mechanisms and Applications, Chem. Rev., 116 (2016) 13279-13412.

[20] H. Huang, J. Huang, Organic and Hybrid Solar Cells, Springer International Publishing2014.

[21] V. Shrotriya, G. Li, Y. Yao, T. Moriarty, K. Emery, Y. Yang, Accurate Measurement and Characterization of Organic Solar Cells, Adv. Funct. Mater., 16 (2006) 2016-2023.

[22] H. Jun, M. Careem, A. Arof, Quantum dot-sensitized solar cells—perspective and recent developments: A review of Cd chalcogenide quantum dots as sensitizers, Renew. Sust. Energ. Rev., 22 (2013) 148-167.

[23] K.C. Vijay, L. Cabau, E. Koukaras, G. Sharma, E. Palomares, Synthesis, optical and electrochemical properties of the A-π-D-π-A porphyrin and its application as an electron donor in efficient solution processed bulk heterojunction solar cells, Nanoscale, 7 (2014) 179-189.

[24] F. Monestier, J.-J. Simon, P. Torchio, L. Escoubas, F. Flory, S. Bailly, R. de Bettignies, S. Guillerez, C. Defranoux, Modeling the short-circuit current density of polymer solar cells based on P3HT:PCBM blend, Sol. Energy Mater. Sol. Cells, 91 (2007) 405-410.

[25] G.F. Burkhard, E.T. Hoke, M.D. McGehee, Accounting for Interference, Scattering, and Electrode Absorption to Make Accurate Internal Quantum Efficiency Measurements in Organic and Other Thin Solar Cells, Adv. Mater., 22 (2010) 3293-3297.

[26] A. Gadisa, M. Svensson, M.R. Andersson, O. Inganäs, Correlation between oxidation potential and open-circuit voltage of composite solar cells based on blends of polythiophenes/ fullerene derivative, Appl. Phys. Lett., 84 (2004) 1609-1611.

[27] K. Vandewal, K. Tvingstedt, A. Gadisa, O. Inganas, J.V. Manca, On the origin of the open-circuit voltage of polymer-fullerene solar cells, Nat Mater, 8 (2009) 904-909.

[28] L.J.A. Koster, V.D. Mihailetchi, R. Ramaker, P.W.M. Blom, Light intensity dependence of open-circuit voltage of polymer:fullerene solar cells, Appl. Phys. Lett., 86 (2005) 123509.

[29] D. Bartesaghi, I.d.C. Pérez, J. Kniepert, S. Roland, M. Turbiez, D. Neher, L.J.A. Koster, Competition between recombination and extraction of free charges determines the fill factor of organic solar cells, 6 (2015) 7083.

[30] A. Mishra, P. Baeuerle, Small Molecule Organic Semiconductors on the Move: Promises for Future Solar Energy Technology, Angew. Chem., Int. Ed., 51 (2012) 2020-2067.

[31] Y. Lin, Y. Li, X. Zhan, Small molecule semiconductors for high-efficiency organic photovoltaics, Chem. Soc. Rev., 41 (2012) 4245-4272.

[32] Z. Li, G. He, X. Wan, Y. Liu, J. Zhou, G. Long, Y. Zuo, M. Zhang, Y. Chen, Solution Processable Rhodanine-Based Small Molecule Organic Photovoltaic Cells with a Power Conversion Efficiency of 6.1%, Advanced Energy Materials, 2 (2012) 74-77.

[33] Z. Wang, Z. Li, J. Liu, J. Mei, K. Li, Y. Li, Q. Peng, Solution-Processable Small Molecules for High-Performance Organic Solar Cells with Rigidly Fluorinated 2,2′-Bithiophene Central Cores, ACS Applied Materials & Interfaces, 8 (2016) 11639-11648.

[34] L. Liang, X.-Q. Chen, X. Xiang, J. Ling, W. Shao, Z. Lu, J. Li, W. Wang, W.-S. Li, Searching proper oligothiophene segment as centre donor moiety for isoindigo-based small molecular photovoltaic materials, Org. Electron., 42 (2017) 93-101.

[35] H. Zhang, Y. Liu, Y. Sun, M. Li, B. Kan, X. Ke, Q. Zhang, X. Wan, Y. Chen, Developing high-performance small molecule organic solar cells via a large planar structure and an electron-withdrawing central unit, Chem. Commun., 53 (2017) 451-454.

[36] J. Hong, J.Y. Choi, T.K. An, M.J. Sung, Y. Kim, Y.-H. Kim, S.-K. Kwon, C.E. Park, A novel small molecule based on dithienophosphole oxide for bulk heterojunction solar cells without pre- or post-treatments, Dyes and Pigments, 142 (2017) 516-523.

[37] K.H. Park, Y.J. Kim, G.B. Lee, T.K. An, C.E. Park, S.-K. Kwon, Y.-H. Kim, Recently Advanced Polymer Materials Containing Dithieno[3,2-b:2′,3′-d]phosphole Oxide for Efficient Charge Transfer in High-Performance Solar Cells, Adv. Funct. Mater., 25 (2015) 3991-3997.

[38] Y. Ren, T. Baumgartner, Combining form with function - the dawn of phosphole-based functional materials, Dalton Transactions, 41 (2012) 7792-7800.

[39] C.-T. Chen, F.-Y. Tsai, C.-Y. Chiang, C.-P. Chen, Spiro-Shaped cis-Stilbene/Fluorene Hybrid Template for the Fabrication of Small-Molecule Bulk Heterojunction Solar Cells, The Journal of Physical Chemistry C, 121 (2017) 15943-15948.

[40] W. Wang, P. Shen, X. Dong, C. Weng, G. Wang, H. Bin, J. Zhang, Z.-G. Zhang, Y. Li, Development of Spiro[cyclopenta[1,2-b:5,4-b′]dithiophene-4,9′-fluorene]-Based A-π-D-π-A Small Molecules with Different Acceptor Units for Efficient Organic Solar Cells, ACS Applied Materials & Interfaces, 9 (2017) 4614-4625.

[41] J. Zhou, X. Wan, Y. Liu, Y. Zuo, Z. Li, G. He, G. Long, W. Ni, C. Li, X. Su, Y. Chen, Small Molecules Based on Benzo[1,2-b:4,5-b′]dithiophene Unit for High-Performance Solution-Processed Organic Solar Cells, J. Am. Chem. Soc., 134 (2012) 16345-16351.

[42] W. Ni, M. Li, X. Wan, H. Feng, B. Kan, Y. Zuo, Y. Chen, A high-performance photovoltaic small molecule developed by modifying the chemical structure and optimizing the morphology of the active layer, RSC Advances, 4 (2014) 31977-31980.

[43] B. Kan, Q. Zhang, M. Li, X. Wan, W. Ni, G. Long, Y. Wang, X. Yang, H. Feng, Y. Chen, Solution-Processed Organic Solar Cells Based on Dialkylthiol-Substituted Benzodithiophene Unit with Efficiency near 10%, J. Am. Chem. Soc., 136 (2014) 15529-15532.

[44] C. Cui, X. Guo, J. Min, B. Guo, X. Cheng, M. Zhang, C.J. Brabec, Y. Li, High-Performance Organic Solar Cells Based on a Small Molecule with Alkylthio-Thienyl-Conjugated Side Chains without Extra Treatments, Adv. Mater., 27 (2015) 7469-7475.

[45] M. Li, F. Liu, X. Wan, W. Ni, B. Kan, H. Feng, Q. Zhang, X. Yang, Y. Wang, Y. Zhang, Y. Shen, T.P. Russell, Y. Chen, Subtle Balance Between Length Scale of Phase Separation and Domain Purification in Small-Molecule Bulk-Heterojunction Blends under Solvent Vapor Treatment, Adv. Mater., 27 (2015) 6296-6302.

[46] K. Sun, Z. Xiao, S. Lu, W. Zajaczkowski, W. Pisula, E. Hanssen, J.M. White, R.M. Williamson, J. Subbiah, J. Ouyang, A.B. Holmes, W.W. Wong, D.J. Jones, A molecular nematic liquid crystalline material for high-performance organic photovoltaics, Nat Commun, 6 (2015) 6013.

[47] Y.-J. Heo, Y.-S. Jung, K. Hwang, J.-E. Kim, J.-S. Yeo, S. Lee, Y.-j. Jeon, D. Lee, D.-Y. Kim, Small Molecule Organic Photovoltaic Modules Fabricated via Halogen-free Solvent

System with Roll-to-roll Compatible Scalable Printing Method, ACS Applied Materials & Interfaces, (2017).

[48] S. Badgujar, G.-Y. Lee, T. Park, C.E. Song, S. Park, S. Oh, W.S. Shin, S.-J. Moon, J.-C. Lee, S.K. Lee, High-Performance Small Molecule via Tailoring Intermolecular Interactions and its Application in Large-Area Organic Photovoltaic Modules, Advanced Energy Materials, 6 (2016) 1600228-n/a.

[49] Y.-Q. Guo, Y. Wang, L.-C. Song, F. Liu, X. Wan, H. Zhang, Y. Chen, Small Molecules with Asymmetric 4-Alkyl-8-alkoxybenzo[1,2-b:4,5-b′]dithiophene as the Central Unit for High-Performance Solar Cells with High Fill Factors, Chem. Mater., 29 (2017) 3694-3703.

[50] N.D. Eastham, A.S. Dudnik, B. Harutyunyan, T.J. Aldrich, M.J. Leonardi, E.F. Manley, M.R. Butler, T. Harschneck, M.A. Ratner, L.X. Chen, M.J. Bedzyk, F.S. Melkonyan, A. Facchetti, R.P.H. Chang, T.J. Marks, Enhanced Light Absorption in Fluorinated Ternary Small-Molecule Photovoltaics, ACS Energy Letters, 2 (2017) 1690-1697.

[51] M.R. Busireddy, N.R. Chereddy, B. Shanigaram, B. Kotamarthi, S. Biswas, G.D. Sharma, J.R. Vaidya, Dithieno[3,2-b:2[prime or minute],3[prime or minute]-d]pyrrole-benzo[c][1,2,5]thiadiazole conjugate small molecule donors: effect of fluorine content on their photovoltaic properties, PCCP, 19 (2017) 20513-20522.

[52] Z. Ji, X. Xu, G. Zhang, Y. Li, Q. Peng, Synergistic effect of halogenation on molecular energy level and photovoltaic performance modulations of highly efficient small molecular materials, Nano Energy, 40 (2017) 214-223.

[53] W. Liu, Z. Zhou, T. Vergote, S. Xu, X. Zhu, A thieno[3,4-b]thiophene-based small-molecule donor with a [small pi]-extended dithienobenzodithiophene core for efficient solution-processed organic solar cells, Materials Chemistry Frontiers, 1 (2017) 2349-2355.

[54] Q. An, F. Zhang, J. Zhang, W. Tang, Z. Deng, B. Hu, Versatile ternary organic solar cells: a critical review, Energy & Environmental Science, 9 (2016) 281-322.

[55] L. Lu, M.A. Kelly, W. You, L. Yu, Status and prospects for ternary organic photovoltaics, Nature Photonics, 9 (2015) 491.

[56] T. Ameri, P. Khoram, J. Min, C.J. Brabec, Organic Ternary Solar Cells: A Review, Adv. Mater., 25 (2013) 4245-4266.

[57] M. Zhang, J. Wang, F. Zhang, Y. Mi, Q. An, W. Wang, X. Ma, J. Zhang, X. Liu, Ternary small molecule solar cells exhibiting power conversion efficiency of 10.3%, Nano Energy, 39 (2017) 571-581.

[58] G. Zhang, K. Zhang, Q. Yin, X.-F. Jiang, Z. Wang, J. Xin, W. Ma, H. Yan, F. Huang, Y. Cao, High-Performance Ternary Organic Solar Cell Enabled by a Thick Active Layer Containing a Liquid Crystalline Small Molecule Donor, J. Am. Chem. Soc., 139 (2017) 2387-2395.

[59] K. Zhu, D. Tang, K. Zhang, Z. Wang, L. Ding, Y. Liu, L. Yuan, J. Fan, B. Song, Y. Zhou, Y. Li, A two-dimension-conjugated small molecule for efficient ternary organic solar cells, Org. Electron., 48 (2017) 179-187.

[60] L. Yang, S. Zhang, C. He, J. Zhang, H. Yao, Y. Yang, Y. Zhang, W. Zhao, J. Hou, New Wide Band Gap Donor for Efficient Fullerene-Free All-Small-Molecule Organic Solar Cells, J. Am. Chem. Soc., 139 (2017) 1958-1966.

[61] B. Qiu, L. Xue, Y. Yang, H. Bin, Y. Zhang, C. Zhang, M. Xiao, K. Park, W. Morrison, Z.-G. Zhang, Y. Li, All-Small-Molecule Nonfullerene Organic Solar Cells with High Fill Factor and High Efficiency over 10%, Chem. Mater., 29 (2017) 7543-7553.

[62] H. Bin, Y. Yang, Z.-G. Zhang, L. Ye, M. Ghasemi, S. Chen, Y. Zhang, C. Zhang, C. Sun, L. Xue, C. Yang, H. Ade, Y. Li, 9.73% Efficiency Nonfullerene All Organic Small Molecule Solar Cells with Absorption-Complementary Donor and Acceptor, J. Am. Chem. Soc., 139 (2017) 5085-5094.

[63] T.J. Aldrich, M.J. Leonardi, A.S. Dudnik, N.D. Eastham, B. Harutyunyan, T.J. Fauvell, E.F. Manley, N. Zhou, M.R. Butler, T. Harschneck, M.A. Ratner, L.X. Chen, M.J. Bedzyk, R.P.H. Chang, F.S. Melkonyan, A. Facchetti, T.J. Marks, Enhanced Fill Factor through Chalcogen Side-Chain Manipulation in Small-Molecule Photovoltaics, ACS Energy Letters, (2017) 2415-2421.

[64] C. Wang, C. Li, S. Wen, P. Ma, G. Wang, C. Wang, H. Li, L. Shen, W. Guo, S. Ruan, Enhanced Photovoltaic Performance of Tetrazine-Based Small Molecules with Conjugated Side Chains, ACS Sustainable Chemistry & Engineering, (2017).

[65] J. Wan, X. Xu, G. Zhang, Y. Li, K. Feng, Q. Peng, Highly efficient halogen-free solvent processed small-molecule organic solar cells enabled by material design and device engineering, Energy & Environmental Science, 10 (2017) 1739-1745.

[66] J.-L. Wang, K.-K. Liu, S. Liu, F. Liu, H.-B. Wu, Y. Cao, T.P. Russell, Applying Thienyl Side Chains and Different π-Bridge to Aromatic Side-Chain Substituted Indacenodithiophene-Based Small Molecule Donors for High-Performance Organic Solar Cells, ACS Applied Materials & Interfaces, 9 (2017) 19998-20009.

[67] J.-L. Wang, K.-K. Liu, S. Liu, F. Xiao, Z.-F. Chang, Y.-Q. Zheng, J.-H. Dou, R.-B. Zhang, H.-B. Wu, J. Pei, Y. Cao, Donor End-Capped Hexafluorinated Oligomers for Organic Solar Cells with 9.3% Efficiency by Engineering the Position of π-Bridge and Sequence of Two-Step Annealing, Chem. Mater., 29 (2017) 1036-1046.

[68] D. Yang, H. Sasabe, T. Sano, J. Kido, Low-Band-Gap Small Molecule for Efficient Organic Solar Cells with a Low Energy Loss below 0.6 eV and a High Open-Circuit Voltage of over 0.9 V, ACS Energy Letters, 2 (2017) 2021-2025.

Highlights

- Highly efficient small organic donor molecules for PV applications have been reviewed.
- Optimization of the important parameters like energy loss and fill factor is discussed.
- Challenges in this area have been discussed.